Presented at the SRI-89 Conference
Berkeley, CA, Aug. 7-11, 1989

BNL-43321

NSLS X-19A Beamline Performance For X-ray Absorption Measurements *

C. Y. Yang+ and J. E. Penner-Hahn
Department of Chemistry, University of Michigan
Ann Arbor, MI 48109

BNL--43321
DE90 001553

P. M. Stefan
National Synchrotron Light Source, Brookhaven National Laboratory
Upton, NY 11973

Characterization of the X-19A beamline at the National Synchrotron Light Source (NSLS) is described. The beamline is designed for high resolution x-ray absorption spectroscopy over a wide energy range. All of the beamline optical components are compatible with ultrahigh vacuum (UHV) operation. This permits measurements to be made in a window-less mode, thereby facilitating lower energy (< 4 KeV) studies. To upgrade the beamline performance, several possible improvements in instrumentation and practice are discussed to increase photon statistics with an optimum energy resolution, while decreasing the harmonic contamination and noise level. A special effort has been made to improve the stability and UHV compatibility of the monochromator system. Initial x-ray absorption results demonstrate the capabilities of this beamline for x-ray absorption studies of low Z elements (e.g. S) in highly dilute systems. The future use of this beamline for carrying out various x-ray absorption experiments is presented.

* Work sponsored by DOE under contract DE-AC02-76CH00016

I. Introduction

Over the past decade, experimental and theoretical advances have made x-ray absorption spectroscopy (XAS) an important quantitative tool for probing the atomic structure, as well as the electronic and vibrational properties, of a wide range materials. With the recent availability of strong and stable synchrotron radiation (SR) sources, the quality of the XAS data has dramatically improved so that complex features and weak signals of higher shells (within ~ 5 Å) of the absorbing atom can be resolved in very dilute or disordered samples, which pose difficulties for other traditional techniques. Many of the available x-ray beamlines at SR sources were initially constructed to serve multiple-purposes, and their designed parameters are, therefore, a compromise between the different types of experimental needs. Using these "standard" XAS lines, it is often quite difficult to measure data for very dilute samples with high energy resolution, and polarization effects in the low x-ray region. In the following, we refer to energies < 4 KeV as low energies. For this reason, an effort has been made to upgrade the X-19A beamline at the NSLS. This beamline is dedicated to XAS measurements over a wide energy range. Particular emphasis has been placed on the low energy range down to the P (2.15 KeV) and S (2.47 KeV) K-absorption edges.

II. Beamline Set Up

In the X-19A beamline, x-rays are transported from the bending magnet source to the measuring apparatus through the system shown in Figure 1. The beamline accepts 3 mrad of horizontal divergence from the source. Many of the primary components, such as the front end, the mirror box, the bender, the photon shutter, and the hutch are based on standard NSLS designs. The first element of the beamline is the white-beam slit. This slit is used to limit the vertical divergence, to exclude scattered radiation, and to control the heat load on the first monochromator crystal. The next element is the silicon carbide rhodium-coated spherical collimating mirror. The mirror is designed to vertically collimate the radiation in order to better match the inherent SR vertical divergence to the acceptance of the monochromator, but it has little effect on the horizontal beam divergence. An incidence angle of 3 mrad was chosen to give a high energy cutoff matched to the K-edge absorption of the rhodium coating at 23 KeV. The collimating mirror is planned as a future addition to the beamline optics. The next element is the white-beam monitor, which operates by detecting the photoelectrons emitted from a tungsten mesh (90% transmittance). In combination with the white-beam slit, this monitor can be used to detect position shifts of the electron beam in the storage ring. The monitor is also used by the monochromator feedback electronics. Downstream of this monitor is the NSLS boomerang-type double flat crystal monochromator [1,2]. After leaving the monochromator, the diffracted x-ray beam from the crystals is sampled by the channel electronic multipler (CEM) monitor. Following the CEM monitor is a cylindrical

aluminum refocusing mirror, which is electroless nickel plated and overcoated with rhodium. This mirror is designed to focus the beam at the sample to a diameter of about 1 mm. The incidence angle of the refocussing mirror is 3 mrad, matching the collimating mirror. The focusing mirror can be dropped out of the beam path for unfocused operation. The next elements are the vertical and horizontal hutch slits located just upstream of the hutch. These slits can also be used to improve the energy resolution and to limit the size of the beam to match the sample size. The following element is the photon shutter, used to stop radiation from going into the hutch. Use of the photon shutter allows other upstream elements to remain illuminated, thus avoiding thermal transients and thereby improving the performance stability of the beamline. The beamline is maintained at ultra-high vacuum UHV up to the 10 mil thick beryllium window located inside the hutch. The beamline is controlled by a Micro-VaxII computer with CAMAC interface running the Micro-VMS operating system. The x-ray absorption data collection software at the X-19A was written by Engbretson [3].

III. Beamline Characterization And Future Improvements

From an experimenter's point of view, the principal concerns for beamline performance are: (1) tunability, (2) available photon fluxes, (3) energy resolution, (4) polarization, and (5) harmonic contamination. The performance of the X-19A beamline is largely determined by the choice of monochromator crystals. The monochromator has two presettable Bragg angle ranges: 8^0 to 15.5^0 and 14.97^0 to 69.14^0. With Si (111) crystals, these angular ranges correspond to two energy ranges of $2.12 < E < 7.93$ KeV and $7.4 < E < 13.53$ KeV respectively. The energy range can be extended to 22.10 KeV with Si (220) crystals. Since the monochromator is installed in a UHV condition, even lower energy operation will be possible in the future. The soft x-ray capability of this beamline could be extended by using large d-spacing crystals [4] such as InSb (111), YB_{66}, and Beryl. Available photon fluxes were calculated using a ray tracing program [5] for Si (111) crystals in an unfocused mode with a 4 x 40 mm^2 beam size at a ring current of 100 mA. The calculated photon fluxes of 10^{10} photons/sec, 5 x 10^{11} photons/sec, and 10^{11} photons/sec are predicted for photon energies at 2.5 KeV, 5 KeV, and 10 KeV respectively. The actual photon fluxes were estimated using an ion chamber with N_2 gas over the energy range 2.5 to 7.9 KeV. The observed photon fluxes are found to be an order of magnitude smaller than the predicated fluxes. A more careful investigation of this is currently underway, and a further optimization of the various beamline components will be conducted. However, the current fluxes of about 10^9 - 10^{10} photons/sec are still adequate to obtain experimental dat with good signal-to-noise in many cases. At the X-19A beamline, two factors contribute to the total energy resolution: the intrinsic reflection width of the monochromator crystals and the angular aperture allowed by the slit systems and the 1/4 mm high source point at the NSLS. The total energy resolution of the

monochromator as a function of energy is shown in Figure 2. As one can see, the energy resolution of Si (111) crystals with a proper slit are well matched to the intrinsic lifetime broadening [6], ΔE_τ, of absorption edges up to 5 KeV. In order to improve the monochromator resolution for energies above 5 KeV, one can use Si (220) crystals. The degree of polarization of the beam was calculated by the same ray tracing procedure [5]. We found that the beam was 98% polarized in the horizontal direction and 2% in the vertical at 10 KeV. The calculation indicated that the degree of polarization should not vary significantly as a function of energy. In general, the harmonic contamination can be reduced by detuning the monochromator. At lower energies, the 10 mil Be window functions as a high-pass filter [7], i.e., to absorb most of the fundamental and to transmit most of the higher order. Thus more detuning is needed to exceed the rocking curve width of the harmonic lines. In lower energy operation, the photon intensity is usually reduced by about 80% to 90% by the detuning procedure. Significant improvement in harmonic rejection will be achieved using a grazing incidence mirror. Gains in intensity by a factor of 3 to 4 may be expected.

IV. Improvements of The Monochromator System

At the X-19A beamline, the monochromator consists of two flat parallel single crystals constrained by a mechanical linkage system. The geometry of the monochromator employs the "right-angle" linkage, which was first developed by Golochenko et al. [1]. With mechanical bearings replacing air bearings, a new UHV compatible version of this type of monochromator was reported by Cowan et al. [2]. Three characteristics of this monochromator are worth mentioning. (A) Ideally, the output beam from the monochromator is fixed in both position and angle as the energy is changed. The major advantage of the fixed exit geometry is to eliminate the need to track the beam motion with post monochromator optics such as a downstream mirror or a table on which the sample and detectors are placed. (B) The monochromator can be operated in UHV. The system can be operated in a window-less beamline, without degrading the storage ring vacuum. (C) Only one motor is needed to produce an energy scan.

There are two practical concerns for this monochromator system: (a) maintaining relative angular alignment during a scan and (2) UHV compatibility. In this type of non-dispersive double-crystal monochromator, the two crystals are arranged to diffract sequentially at the same Bragg angle. The throughput of monochromator is a convolution of the rocking curves of the individual crystals. Thus, misalignment of the relative angle from parallelism between the two crystals will lead to a significant loss of intensity. Ideally, it is desirable to maintain parallelism of the crystals. In other words, the crystals would simply remain parallel, without additional effort. Unfortunately, errors induced by the mechanical slides tend to increase with the length of travel, and thus for large angular scans, it is difficult to maintain sufficient

angular alignment between the two crystals. Over the angular range from 14^0 to 70^0, the angular error in crystal parallelism is about 30 arcseconds due to the tolerances of the system. Furthermore, two general problems associated with the properties of crystals and the nature of SR are anticipated, which can strongly affect the alignment of the crystals. First, the monochromator crystals not only reflect the fundamental, but also higher orders. In order to filter out unwanted reflections, higher harmonics can be suppressed by adjusting the pair of crystals to be slightly non-parallel. For example, with Si (111) crystals at 10 KeV, the intensity of the third harmonic can be reduced by 10^{+3} with an angular deviation ca. 4 arcseconds. Although the current monochromator has a water-cooled front crystal, the problem of considerable heat loading on the first crystal (~ 50^0 C) in the white beam still exists. This can change lattice constants of the two crystals due to different thermal expansion. Based on the above considerations, continual angular correction for this type of monochromator is essential to proper beamline operation.

In practice, piezoelectric transducers (PZT's) with an analog feedback control circuit are used to apply a correction angle or fine tuning to the second crystal. After the Bragg angle of the first crystal is set to the desired energy, the PZT mechanism gives the second crystal two additional angular degrees of freedom. These control to relative angle between the two crystals and the alignment of the netplanes perpendicular to the reflection plane. The former is the most critical adjustment. This is achieved by operating on the side of the rocking curve of the second crystal as a function of the relative angular alignment over a small range, i.e., to look at the reflected intensity from the monochromator as a function of the voltage applied to the second crystal PZT. The analog feedback system used to control the PZT bias is modeled on the system described by Krolzig, et al [8]. It monitors the efficiency of the monochromator by forming the ratio of two signals, one proportional to the white beam flux entering the monochromator, and a second proportional to monochromatic output flux. In our case, the signals measured by the white-beam monitor and the ion chamber in the hutch are used as input signals for the feedback system. The PZT bias is varied by a d.c. feedback circuit to hold the ratio of these signals equal to a reference signal. This approach easily permits detuning for harmonic rejection, and works well at maintaining a constant output flux from the monochromator during an XAS scan.

One characteristic of this monochromator is that it operates in UHV. To achieve UHV compatibility, the internal bearings of the monochromator could not be lubricated with oils or greases. However, we had difficulty in operating the monochromator for more than about one month without encountering a bearing failure. This problem now appears to be resolved, after we conducted separate UHV tests of commercial stainless steel bearings with and without UHV-compatible dry lubricants. In our case, the fit of the bearings in the monochromator mechanism seemed crucial; the bearing must fit onto its shaft and into its housing using only light finger

pressure. Also, the dry lubricant must be very thin, to prevent removal of all radial free play in the un-loaded bearing.

V. Initial X-ray Absorption Results

The capabilities of this beamline for x-ray absorption studies are illustrated by the spectra in Figures 3 and 4. The energy resolution of the monochromator was tested by measuring the Mn K-edge of $KMnO_4$ as shown in Figure 3 using Si (111) crystals with a 0.5 mm slit. We estimate the experimental monochromator resolution (Figure 3) to be ca.1.5 eV, as predicted in Figure 2. Higher-resolution edge spectra could be obtained by using crystals with higher index diffraction planes with an optimum slit setting. An EXAFS spectrum and its corresponding k^2 Fourier transform of S K-edge of S_8 [10% atomic weight in BN_3] are shown in Figure 4. The EXAFS spectrum was measured using Si (111) crystals. The monochromator was detuned ca. 80%. The beam size was approximately 4 x 20 mm^2, and the intensity was estimated to be ca. 10^8 photons/sec. The data was collected using an ion chamber fluorescence detector [9] with 1 sec acquisition time per data point. Other good signal-to-noise ratio sulfur edge spectra for highly dilute systems are also published in this volume [7]. During this run, the NSLS was operated at an energy of 2.5 GeV and electron current from 200 to 90 mA. Due to the brightness of the NSLS x-ray ring and the existing experimental setup of the X-19A beamline, we feel that high quality fluorescence EXAFS spectra for low Z elements (P, S, and Cl) can be obtained in reasonable time for lower concentration samples of ca. 0.01% atomic weight.

VI. Further Applications

This beamline was designed for high resolution XAS measurements over a wide energy range. Initial results demonstrate that with a further improvement of the monochromator, this goal has been accomplished. A unique feature of this beamline is its UHV compatibility. In its current configuration, the single thick Be window absorbs ca. 95% of the photons at 2.5 KeV. Despite this limitation, we obtained a good signal-to-noise ratio for dilute samples comparable to that reported using the SSRL 54-pole undulator [10]. In the future, the Be window will be either removed (for UHV compatible samples) or replaced with a thin diamond window to permit even lower energy studies. This will open a new spectroscopic window for studies of samples of biological, chemical, and materials science interest in an energy range (1-3 KeV).

Acknowledgments

We wish to thank Steve Heald and Daniel Fischer for helpful discussions. Support for this research was provided by the Office of the Vice President for Research, University of Michigan, and the U.S. Department of Energy under contract NO. DE-AC02-76CH0016.

Figure Captions

Figure 1 Layout of the key components of the X-19A beamline at the NSLS.

Figure 2 Expected energy resolution of the monochromator for Si (111) and Si(220) crystals with different slit sittings.

Figure 3 Near-edge spectrum of Mn K-edge of $KMnO_4$, measured with Si (111) crystals and a slit of o.5mm. From this measurement we estimate the resolution of the monochromator is ca. 1.5 eV, as expected.

Figure 4 Fourier transform of S_8 [10% atomic weight in BN_3]. The k^2 transform was taken over a k-space region of 2 to 10 $Å^{-1}$. The inset shows the quality of EXAFS data.

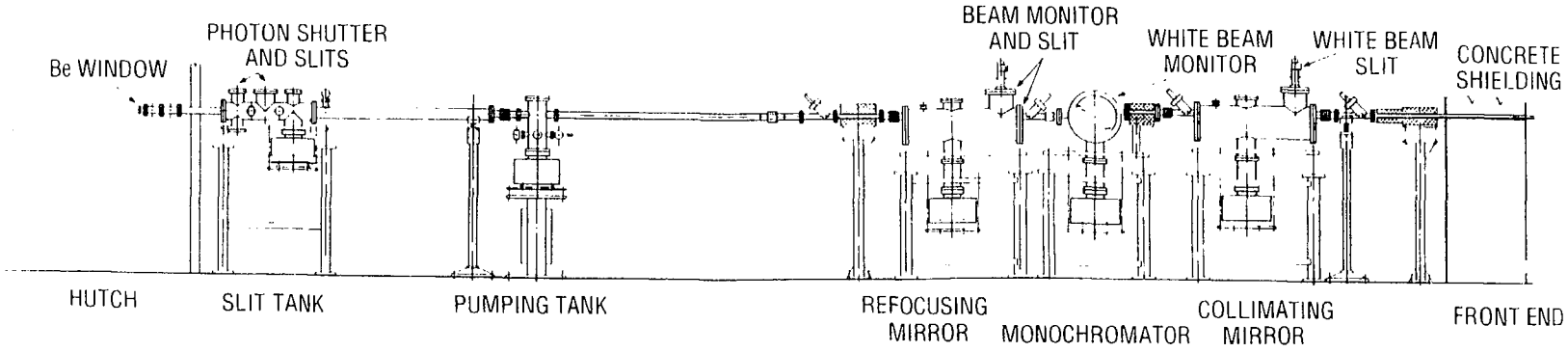

Fig 1 Yang et al

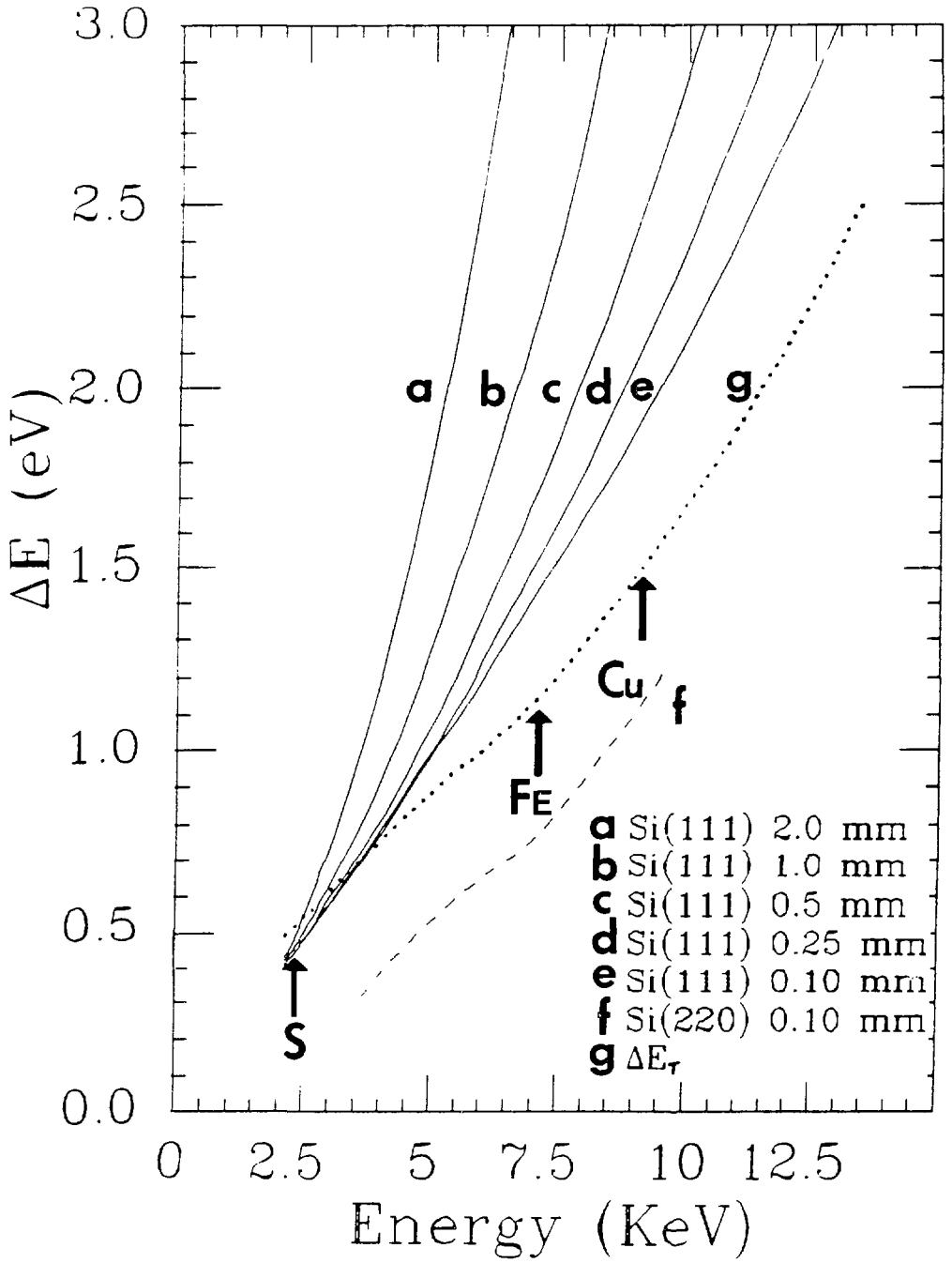

Figure 2
YANG et al

References

+ Corresponding Address: Bldg. 480 Brookhaven National Lab. Upton, NY 11973

1. J. A. Golovchenko, R. A. Levesque and P. L. Cowan, Rev. Sci. Instrum. 52 (1981) 509.
2. P.L. Cowan, J. B. Hastings, T. Jach and J. P. Kirkland, Nucl. Instr. and Meth. 208 (1983) 349.
3. M. Engbretson, unpublished.
4. J. Wong et al., Nucl. Inst. and Meth. 195 (1982) 133.
5. S. M. Heald and J. B. Hastings, Nucl. Instr. and Meth. 187 (1981) 553.
6. M. H. Chen and B. Crasemann, Phys. Rev. A 21 (1980) 436, and references therein.
7. D. A. Fischer and C. Y. Yang, to be published in this Volume.
8. A. Krolzig, G. Materlik, M. Swars and J. Zegenhagen, Nucl. Instr. and Meth. 219 (1984) 430.
9. F. E. Lytle et al., Nucl. Instr. and Meth. 226 (1984) 542.
10. B. Hedman et al., Nucl. Instr. Meth. A246 (1986) 797.

Figure 3

Yang et al

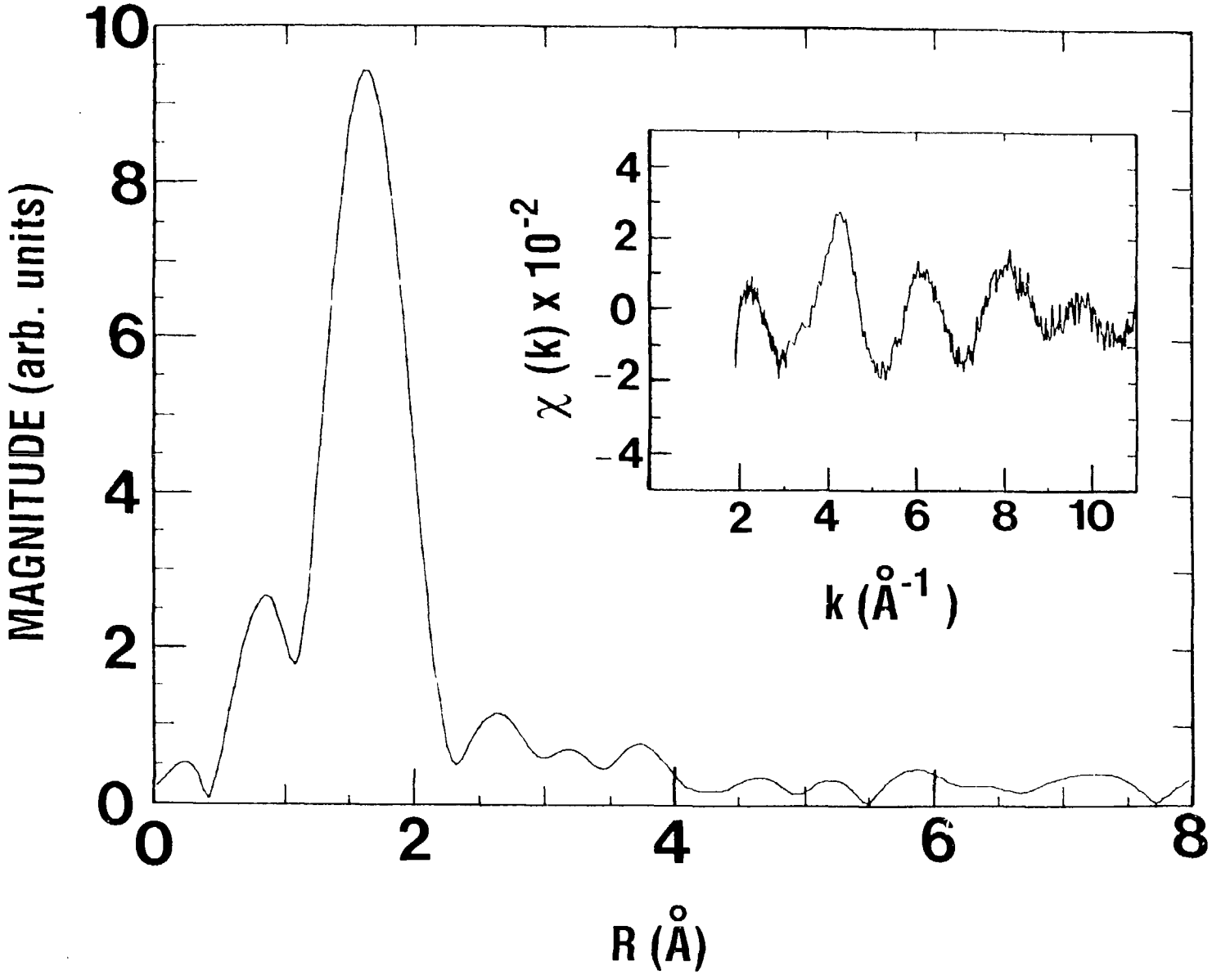
MAGNITUDE (arb. units)
R (Å)
χ (k) x 10^-2
k (Å^-1)